

# Isotope shifts of the $(3s3p)^3P_{0,1,2} - (3s4s)^3S_1$ Mg I transitions

Ming He, Kasper T. Therkildsen, Brian B. Jensen, Anders Brusch, and Jan W. Thomsen  
The Niels Bohr Institute, Universitetsparken 5, 2100 Copenhagen, Denmark

Sergey G. Porsev<sup>y</sup>

Petersburg Nuclear Physics Institute, Gatchina, Leningrad district 188300, Russia  
(Dated: February 21, 2024)

We report measurements of the isotope shifts of the  $(3s3p)^3P_{0,1,2} - (3s4s)^3S_1$  Mg I transitions for the stable isotopes  $^{24}\text{Mg}$  ( $I=0$ ),  $^{25}\text{Mg}$  ( $I=5/2$ ) and  $^{26}\text{Mg}$  ( $I=0$ ). Furthermore the  $^{25}\text{Mg}$   $^3S_1$  hypernecoefficient  $A(^3S_1) = (-321.6 \pm 1.5) \text{ MHz}$  is extracted and found to be in excellent agreement with state-of-the-art theoretical predictions giving  $A(^3S_1) = -325 \text{ MHz}$  and  $B(^3S_1) \sim 10^5 \text{ MHz}$ . Compared to previous measurements, the data presented in this work is improved up to a factor of ten.

PACS numbers: Valid PACS appear here

## I. INTRODUCTION

Accurate measurements of atomic transitions play an important role in many parts of physics and astronomy. They form a basis for state-of-the-art atomic structure calculations and provide important reference data for spectroscopic measurements. Accurate spectroscopic measurements have a wide range of applications covering astrophysical [1] and laboratory based experiments including optical cooling schemes and atomic clocks [2, 3]. With the access to new and improved spectroscopic data detailed models using relativistic many-body methods of atomic structure calculations and models may advance significantly [4, 5]. For the alkaline earth elements some transitions are very well known, but most transitions are relatively unknown or known only with a modest accuracy.

Thermagnesium atom is particularly interesting in connection with star evolution and for accurate spectroscopic measurements on distant quasars in the search for a possible temporal drift of the fine structure constant  $\alpha = e^2/\hbar c$ . For star evolution models the  $(3s3p)^3P_{0,1,2} - (3s4s)^3S_1$  transitions play an important role and here new data on the isotope shifts will be helpful [1]. Absorption measurements from distant quasars rely on accurate laboratory values of transition wavelengths and isotope ratios.

In this Brief Report we present new improved measurements for the isotope shift and hyperne structure splitting of the  $(3s3p)^3P_{0,1,2} - (3s4s)^3S_1$  Mg I transitions around 517 nm in a metastable atomic magnesium beam. We improve previous measurements by up to a factor of ten for the stable isotopes  $^{24}\text{Mg}$  ( $I=0$ ),  $^{25}\text{Mg}$  ( $I=5/2$ ) and  $^{26}\text{Mg}$  ( $I=0$ ). For  $^{25}\text{Mg}$   $^3S_1$  we extract the hypernecoefficient  $A(^3S_1)$  and compare the result to state-of-the-art

relativistic many-body calculations.

## II. EXPERIMENTAL SETUP

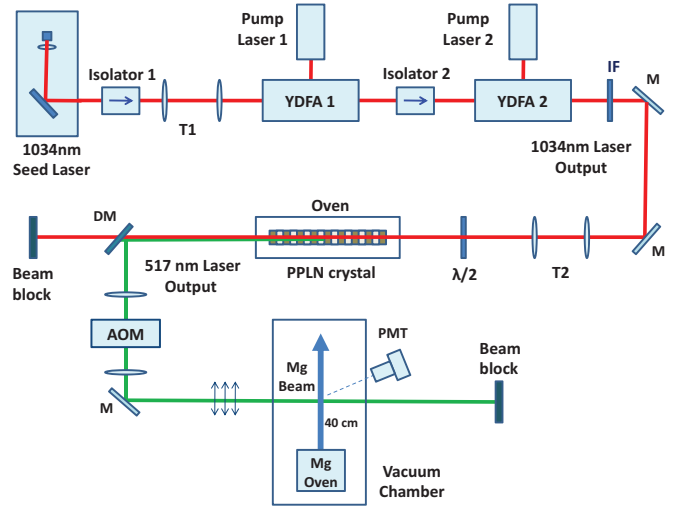


FIG. 1: (color online) Schematic diagram of the laser system: T, telescope; DM, dichroic mirror; IF, interference filter; M, mirror;  $\lambda/2$ , half waveplates; BS, beam splitter; AOM, acousto-optic modulator; PMT, photomultiplier tube. A two-stage YDFA system is used for 1034 nm laser amplification, and is single pass frequency doubled in a PPLN crystal. Fluorescence spectroscopy is performed on a metastable magnesium beam, approximately 40 cm from the oven orifice.

Fig. 1 shows the experimental setup used for spectroscopy on metastable magnesium atoms. The Mg oven is operated around 520 °C and produces an effusive magnesium beam with mean velocity 1000 m/s and flux of  $10^{13}$  atom/s. Electron impact initiates the discharge which runs at a stable current of about one ampere in a setup similar to the one described in [6]. Using the main  $285.3 \text{ nm } (3s^2)^1S_0 - (3s3p)^1P_1$  transition we estimate about 40% of the atoms are in a metastable state,

<sup>y</sup>Present address: School of Physics, University of New South Wales, Sydney, NSW 2052, Australia.  
Electronic address: kaspertt@fys.ku.dk

distributed among the  $^3P_{0,1,2}$  levels. The 517 nm light is produced from a fiber amplified diode laser centered at 1034 nm. We use an external cavity diode laser in a Littrow configuration followed by a 40 dB optical isolator. Typically the output after the isolator is 15 mW and about 10 mW is injected into a two-stage Yb-doped fiber amplifier (YDFA) system. The fiber consists of a highly doped single-mode core of 10  $\mu$ m diameter with a peak absorption of 1200 dB/m at 976 nm and a large multimode pump guiding cladding of 125  $\mu$ m in diameter. The fibers are pumped with up to 5 W at 976 nm. After the amplifier stage 1.5 W of 1034 nm light is generated. The 1034 nm light is single pass frequency doubled in a periodically poled lithium niobate (PPLN) crystal generating up to 40 mW at 517 nm. The domain period of the PPLN crystal is 6.37  $\mu$ m with a quasi-phase matching temperature around 35  $^{\circ}$ C and temperature coefficient of 0.09 nm/K. An oven is used to stabilize the PPLN temperature within 0.01  $^{\circ}$ C in order to achieve optimal phase matching. After the frequency doubling, a dichroic mirror is used to separate the 517 nm light from the 1034 nm light.

Spectroscopy is performed 40 cm from the oven orifice using linearly polarized light. The imaging system collects fluorescence from an area of about 8 mm<sup>2</sup> within the atomic beam limiting the residual Doppler effect to 60 MHz. A 275 MHz – 400 MHz AOM is used for frequency scale calibration. The absolute AOM frequency is controlled below 1 kHz RMS and was verified using a precision counter. For calibration both zero and first order beams from the AOM are overlapped producing a double set of spectra. Changing the dc offset of the AOM enable us to test the degree of linearity of the frequency scan. The intrinsic linewidth of the 517 nm light has been measured to be below 3 MHz using a high-finesse cavity. Each spectrum is averaged 32 times and 30 different spectra are recorded for each transition.

### III. METHOD OF CALCULATION

The method used for calculation of the magnetic dipole and electric quadrupole hyperfine structure constants A and B for the  $^3S_1$  state is a combination of the configuration interaction (CI) method with many-body perturbation theory (MBPT) [7]. Initially the method was developed for calculating energy levels. The MBPT was used to construct an effective Hamiltonian for valence electrons. Then the multiparticle Schrödinger equation for valence electrons was solved in the frame of the CI method. Following the earlier works, we refer to this approach as the CI+MBPT formalism.

In this approach, the energies and wave functions are determined from the equation

$$H_e(E_n)|n\rangle = E_n|n\rangle;$$

where the effective Hamiltonian is defined as

$$H_e(E) = H_{FC} + \langle E \rangle;$$

Here  $H_{FC}$  is the Hamiltonian in the frozen core approximation and  $\langle E \rangle$  is the energy-dependent correction, which takes into account virtual core excitations.

In order to calculate other atomic observables, one needs to construct the corresponding effective operators for valence electrons [8, 9, 10]. In particular, the effective operator of the hyperfine interaction used in this work accounts for the core-valence and core-core correlations. To account for shielding of an externally applied field by core electrons we have solved random-phase approximation (RPA) equations, summing a certain sequence of many-body diagrams to all orders of MBPT [8, 11].

We consider Mg as a two-electron atom with the core  $[1s^2, \dots, 2p^6]$ . On the whole the one-electron basis set for Mg consists of  $1s\{13s, 2p\{13p, 3d\{12d, \text{ and } 4f\{11f$  orbitals, where the core- and 3s, 3p, 3d, and 4f orbitals are Dirac-Hartree-Fock (DHF) ones, while all the rest are the virtual orbitals. The orbitals  $1s\{3s$  are constructed by solving the DHF equations in  $V^N$  approximation, 3p orbital is obtained in  $V^{N-1}$  approximation, and 4s, 4p, 3d, and 4f orbitals are constructed in  $V^{N-2}$  approximation. We determined virtual orbitals using a recurrent procedure similar to Ref. [12] and described in detail in [9, 10]. Configuration-interaction states were formed using this one-particle basis set which is sufficiently large to obtain numerically converged CI results. An extended basis set, used at the stage of MBPT calculations, included  $1s\{19s, 2p\{19p, 3d\{18d, 4f\{15f, \text{ and } 5g\{11g$  orbitals.

The results obtained in the frame of the CI+MBPT method for the hfs constants A and B are  $A(^3S_1) = -325$  MHz and  $B(^3S_1) = 10^{-5}$  MHz. The theoretical value for the magnetic dipole constant A is in a good agreement with the experimental value obtained in this work  $A(^3S_1) = -321.6 \pm 1.5$  MHz.

The electric quadrupole hfs constant  $B(^3S_1)$  is very close to zero. In the absence of configuration interaction of the 3s4s configuration with other configurations (like 3snd and  $nd^2$  configurations, where  $n \geq 3$ ) the hfs constant B would be exactly equal to zero. But (very weak) configuration interaction leads to a non-zero value of B, though very small.

### IV. RESULTS AND DISCUSSION

Figs. 2, 3 and 4 show typical fluorescence spectra as a function of laser frequency for the  $^3P_{0,1,2} - ^3S_1$  transitions. The blue curve is the raw data and the red curve is a Voigt profile fit to the data. For  $^{24}\text{Mg}$  we obtain a FWHM linewidth of 55 MHz in agreement with our beam and detector geometry. From the spectra we clearly identify the isotope shift and the hyperfine components  $(^3P_{0,1,2})_F - (^3S_1)_F$  of  $^{25}\text{Mg}$ . Data for the hyperfine coefficients of the  $^3P_{1,2}$  levels are needed to extract the hyperfine coefficient  $A(^3S_1)$  and are taken from [13]. We extract the hyperfine coefficient  $A(^3S_1) = (-321.6 \pm 1.5)$  MHz. As described in Sec. III the electric quadrupole hfs

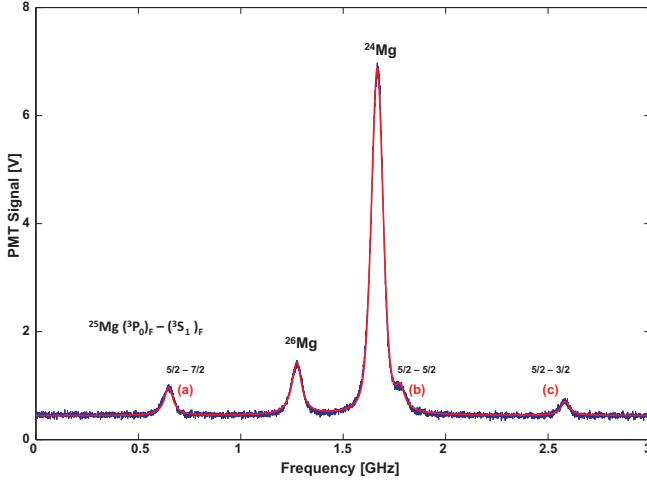


FIG. 2: (color online) Fluorescence signal from the  $^3P_0 - ^3S_1$  transition. The blue curve represents the experimental data and the red curve is a fit to the data. The hyperfine splitting of  $^{25}\text{Mg } (^3P_0)_F - (^3S_1)_F$  are indicated as (a) - (c).

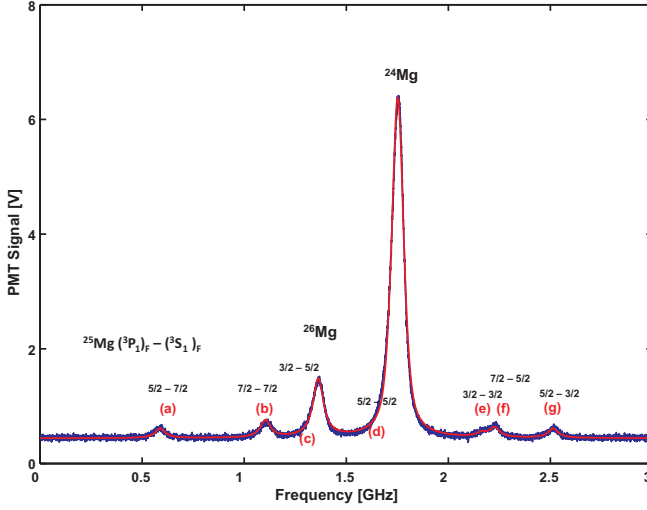


FIG. 3: (color online) Fluorescence signal from the  $^3P_1 - ^3S_1$  transition. The blue curve represents the experimental data and the red curve is a fit to the data. The hyperfine splitting of  $^{25}\text{Mg } (^3P_1)_F - (^3S_1)_F$  are indicated as (a) - (g).

constant  $B(^3S_1)$  is significantly smaller than the resolution of the experiment and is therefore set to zero in the fitting procedure. Table I summarizes our findings and compares with previous measurements. Different systematic errors have been investigated as mentioned in Sec. II, all of which have been determined to be lower than the statistical error. Errors listed in Table I are pure statistical errors. Here it can be seen that the value for the hyperfine coefficient  $A(^3S_1)$  and the isotope shifts agree with previous measurements within the uncertainty.

We observe the  $^{24}\text{Mg} - ^{26}\text{Mg}$  shift to be almost constant which indicates that relativistic isotope shift effects are

small or comparable to the statistical error in our mea-

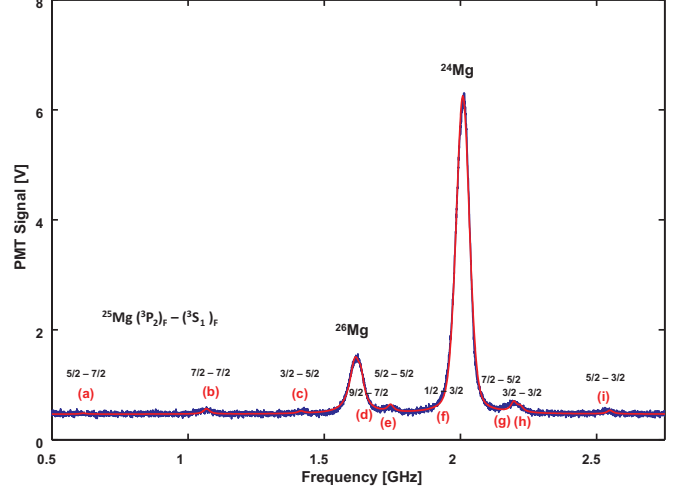


FIG. 4: (color online) Fluorescence signal from the  $^3P_2 - ^3S_1$  transition. The blue curve represents the experimental data and the red curve is a fit to the data. The hyperfine splitting of  $^{25}\text{Mg } (^3P_2)_F - (^3S_1)_F$  are indicated as (a) - (i).

surement.

Our measured isotope shifts are accounted for by pure mass effect. In this case the ratio between the  $^{24}\text{Mg} - ^{26}\text{Mg}$  and  $^{24}\text{Mg} - ^{25}\text{Mg}$  shifts can be expressed as [15]:

$$\frac{(^{24}\text{Mg} - ^{26}\text{Mg})}{(^{24}\text{Mg} - ^{25}\text{Mg})} = \frac{26}{26} \frac{24}{24} \frac{25}{25} \frac{24}{24} = \frac{25}{13}, \quad 1.92 : (1)$$

We obtain the ratios:  $^3P_0 - ^3S_1$  1.90 ± 0.02,  $^3P_1 - ^3S_1$  1.87 ± 0.01 and  $^3P_2 - ^3S_1$  1.92 ± 0.01. These values are consistent with previous results [15, 16].

## V. CONCLUSION

In this paper we present improved data for the isotope shift of the  $\text{Mg } ^3P_{0,1,2} - ^3S_1$  and the hyperfine coefficient  $A(^3S_1)$  for the  $^{25}\text{Mg}$  isotope. We find good agreement between state of the art many body theory and experimental results. Experimental values reported here are improved by up to a factor of ten compared to previous studies.

## Acknowledgments

We would like to acknowledge financial support from the Lundbeck foundation and the Carlsberg foundation. The authors also gratefully acknowledge Kjeld Jensen for technical assistance and Julian Berengut for editing the manuscript.

	$^3P_0 - ^3S_1$		$^3P_1 - ^3S_1$		$^3P_2 - ^3S_1$		
	$^{24} \text{Mg}$ [MHz]	$^{25} \text{Mg}$ [MHz]	$^{24} \text{Mg}$ [MHz]	$^{25} \text{Mg}$ [MHz]	$^{24} \text{Mg}$ [MHz]	$^{25} \text{Mg}$ [MHz]	A ( $^3S_1$ ) [MHz]
Ref. [14] (1949)	414 9		366 45		414 12		-322 6
Ref. [15] (1978)	396 6	210 36	391 4.5	201 21	393 7.5	204 7.5	-329 6
Ref. [16] (1990)	391 10	214 10	393 10	215 10	397 10	217 10	-322 6
This work (2009)	391.3 1.7	205.7 1.5	390.1 1.4	209.1 1.3	394.4 0.8	205.7 0.8	-321.6 1.5

TABLE I: Measured isotope shift and  $^3S_1$  hyperfine structure constant. The errors listed are the statistical errors.

- 
- [1] M. A. Denius, J. D. Tanner, S. Johansson, H. Lundberg, S. G. Ryan, *Astron. and Astrophys.* 461, 767 (2007)
- [2] T. Rosenband, D. B. Hume, P. O. Schmidt, C. W. Chou, A. Brusch, L. Lorini, W. H. Oskay, R. E. Dullinger, T. M. Fortier, J. E. Stalnaker et al., *Science* 319, 1808 (2008).
- [3] A. D. Ludlow, T. Zelevinsky, G. K. Campbell, S. Blatt, M. M. Boyd, M. H. G. de Miranda, M. J. Martin, J. W. Thomsen, S. M. Foreman, J. Ye et al., *Science* 319, 1805 (2008).
- [4] J. C. Berengut, V. V. Flambaum, and M. G. Kozlov, *Phys. Rev. A* 72, 044501 (2005).
- [5] J. C. Berengut, V. A. Dzuba, V. V. Flambaum, and M. G. Kozlov, *Phys. Rev. A* 69, 044102 (2004).
- [6] G. Giusfredi, A. Godone, E. Bava, and C. Novero, *J. Appl. Phys.* 63, 1279 (1988).
- [7] V. A. Dzuba, V. V. Flambaum, and M. G. Kozlov, *Phys. Rev. A* 54, 3948 (1996).
- [8] V. A. Dzuba, M. G. Kozlov, S. G. Porsev, and V. V. Flambaum, *Zh. Eksp. Teor. Fiz.* 114, 1636 (1998), [*Sov. Phys. JETP* 87 885, (1998)].
- [9] S. G. Porsev, Yu. G. Rakhlin, and M. G. Kozlov, *Phys. Rev. A* 60, 2781 (1999).
- [10] S. G. Porsev, Yu. G. Rakhlin, and M. G. Kozlov, *J. Phys. B* 32, 1113 (1999).
- [11] D. Kolb, W. R. Johnson, and P. Shorer, *Phys. Rev. A* 26, 19 (1982).
- [12] P. Bogdanovich and G. Žukauskas, *Sov. Phys. Collect.* 23, 13 (1983).
- [13] A. Lurio, *Phys. Rev.* 126, 1768 (1962).
- [14] M. F. Crawford, F. M. Kelly, A. L. Schawlow, W. M. Gray, *Phys. Rev.* 76, 1527 (1949).
- [15] L. Hallstadius and J. E. Hansen, *Z. Phys. A* 285, 365 (1978).
- [16] C. Novero and A. Godone, *Z. Phys. D* 17, 33 (1990).